

Synthesis of nanometer-sized hematite single crystals through NAC-FAS method

M. IWASAKI*, M. HARA, S. ITO

*Department of Applied Chemistry, Faculty of Science and Engineering,
Kinki University, 3-4-1 Kowakae, Higashi-osaka, Osaka 577-8502, Japan
E-mail: m-iwa@apch.kindai.ac.jp*

Nanometer-sized spherical hematite single crystals were prepared by heating the precipitate which was synthesized from $\text{Fe}(\text{OH})(\text{CH}_3\text{COO})_2$ and NaOH in alkaline ethanol-water solutions without the deliberate addition of surfactants or adsorbing ligands. Hematite nanocrystals (5–10 nm in diameter) and ferrihydrite (<5 nm) were obtained from the mixture of $\text{H}_2\text{O}/\text{EtOH}$ (R_s) = 100 ml/100 ml as a initial medium, whereas goethite, hematite (20–40 nm), and ferrihydrite were precipitated at R_s = 200/0. Adsorbing ligands such as acetoxy groups and ethanol on particles retarded the hematite growth and goethite formation. TEM observation of the particles prepared at R_s = 100/100 with heat treatment at 400 °C for 2 hours showed them consisting of single spherical hematite crystals 22 nm in mean diameter with narrow size distribution. Various individual effects were investigated for their contributions to crystal structure and size of precipitates ; they included NaOH to $\text{Fe}(\text{OH})(\text{CH}_3\text{COO})_2$ ratio, solvent, dropping rate of alkaline solution, and aging time.

© 2000 Kluwer Academic Publishers

1. Introduction

Nanometer-scale materials are of interest since their diversity of properties is a function of particle size and geometry. Specific surface area is one of the important factors for determining the application of the nanocrystalline materials as sensors and catalysts. Catalysis activity strongly depends on the particle size, crystal structure, and morphology. Therefore their properties should be strictly controlled in order to increase their (photo)catalytic effect. Nanocrystallite hematite ($\alpha\text{-Fe}_2\text{O}_3$) particles are also in demand as catalysts and photocatalysts [1, 2]. Moreover, $\alpha\text{-Fe}_2\text{O}_3$ shows better photoelectrochemical response at longer wavelengths in the visible region because it has a narrower band gap than that of TiO_2 [2].

Much literature has been published describing the preparation of hematite particles [3–24]. Their properties such as chemical and structural composition, particle size, morphology, color, magnetic quality, and other characteristics are strongly influenced by a variety of preparation parameters including pH, temperature, time of aging, concentration of reacting species, and nature of anions [3–7]. Hematite crystal is generally prepared via ferrihydrite in neutral to alkaline media or by forced hydrolysis of acid solution with iron (III) salt.

In alkaline media, hematite particle size and morphology are changed by various conditions. Hematite forms rods, often with fibrous ends, in the presence of citrate or maltose at pH 11 and 80 °C [8]. Rhombohedral

hematites are formed at pH 12.2 and 70 °C in the presence of Cu ions [9]. Much larger hematite hexagonal plate crystals form under hydrothermal conditions in the presence of triethanolamine in strongly alkaline media [10].

Recently, nanocrystalline ferric (hydrous) oxides were synthesized in solutions and in films. Rhombohedral hematite crystals of 50–100 nm in diameter were prepared by forced hydrolysis of iron (III) salts at 98 °C under the appropriate preparation conditions for anion type, concentration of ferric salt, and acidity [11, 12]. Some researchers have incorporated nanocrystalline ferric (hydrous) oxides particles into Langmuir-Blodgett (LB) film using surfactant [13, 14].

We have investigated the synthesis of nanocrystalline ZnO and TiO_2 particles through the NAC-FAS (NAnometer-sized Crystal Formation in Alcoholic Solutions) method, in which an alcohol-water mixture with metal salts is refluxed without the deliberate addition of surfactants or adsorbing ligands [25–27].

In this study, the preparation of nanometer-sized hematite ($\alpha\text{-Fe}_2\text{O}_3$) single crystals was investigated by the NAC-FAS method using ferric basic acetate ($\text{Fe}(\text{OH})(\text{CH}_3\text{COO})_2$). Various results about the crystal structure, size, and form of the particles against the NaOH to $\text{Fe}(\text{OH})(\text{CH}_3\text{COO})_2$ ratio, the alcohol to water ratio, and the aging time were also demonstrated with powder X-ray diffraction and transmission electron microscope.

* Author to whom all correspondence should be addressed.

2. Experimental

Ferric basic acetate ($\text{Fe}(\text{OH})(\text{CH}_3\text{COO})_2$; reagent-grade; 4.77 g, 25 mmol) was dissolved in 200 ml of ethanol-water mixture at 70 °C. The volume fraction of water to ethanol ($\text{H}_2\text{O}/\text{EtOH}$; abbreviated to Rs) was varied from 0/200 to 200/0. Next, 100 ml of ethanolic solution containing sodium hydroxide was added dropwise to the solution. The rate of this dropwise addition was adjusted from 200 ml min^{-1} to 1.67 ml min^{-1} . The molar ratio of sodium hydroxide to ferric basic acetate (designated as Rc) was varied from 0.5 to 4. After being refluxed for a predetermined time (1 to 48 hours), the mixture was cooled to room temperature while stirring the mixture. Precipitates in the reaction mixture were isolated by centrifugal separation at a rotating rate of 10,000 r.p.m., washed with methanol, and dried at room temperature overnight in a vacuum.

Powder X-ray diffraction (XRD; RIGAKU RINT 2000) was carried out using Ni-filtrated $\text{Cu-K}\alpha$ radiation for determining the crystal structure of products. The crystallite size was calculated from the half-peak width at half-height for the hematite (104) diffraction peak using the Scherrer equation. The particle size was observed using a transmission electron microscope (TEM : JEOL JEM-3010) at an acceleration voltage of 300 kV. Specific surface area was calculated using the Brunauer-Enarmett-Teller (BET) method. Differential thermal analysis attached with thermogravimetry were carried out using Rigaku TG8101D from room temperature to 700 °C at a rate of increase of 10 °C min^{-1} under an air stream. FT-IR spectra were obtained on Perkin-Elmer 1760 by using the diffuse reflection method.

3. Results and discussion

Precipitates obtained by centrifugal separation were a dark red soft powder in all preparation conditions. Crystal form and crystallite size of the products strongly depended on sample preparation conditions such as Rc and Rs in media, reflux time, and dropping rate of NaOH-containing ethanol.

3.1. Effect of NaOH to $\text{FeOH}(\text{CH}_3\text{COO})_2$ ratio

Fig. 1 shows the XRD patterns for the products prepared in the water-ethanol mixture ($R_s = 100/100$) at $R_c = 0.5$ (a), 1 (b), 2 (c), and 4 (d). In the patterns (a), (b), and (c), all the sharp peaks were identified as hematite ($\alpha\text{-Fe}_2\text{O}_3$; Joint Committee on Powder Diffraction Standard (JCPDS) Card No. 33-0664). Broad peaks located around $2\theta = 35$ and 62 degrees are similar to those of 2-line ferrihydrite. The peaks due to hematite, ferrihydrite, and goethite ($\alpha\text{-FeOOH}$; JCPDS Card No. 29-0713) appeared in the pattern (d). The diffraction peaks of hematite crystal became broader as Rc was increased. The crystallite size of hematite particles calculated from the Scherrer equation for the products (a), (b), and (c) was 31, 26, and 18 nm, respectively. Since the products had a high specific surface area (250–330 $\text{m}^2 \text{g}^{-1}$), the hematite particles probably consist of nanometer-sized crystalline. The crystallite size decreased with increasing Rc, indicating that NaOH retarded the growth of hematite particles and accelerated goethite formation.

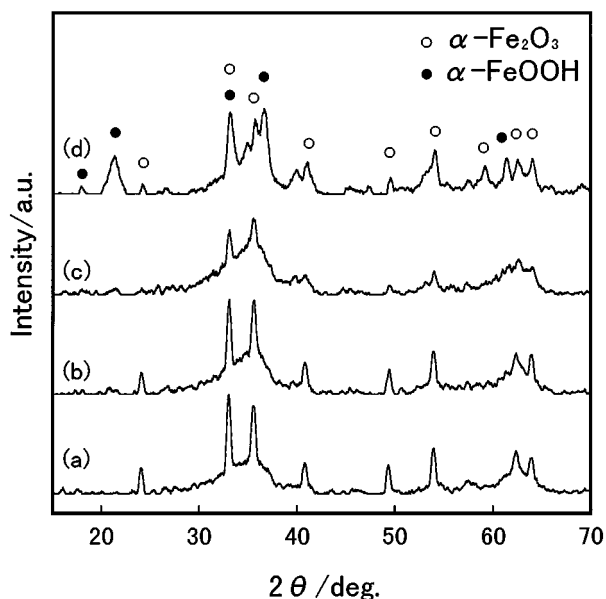


Figure 1 XRD patterns for the products prepared at various NaOH to $\text{FeOH}(\text{CH}_3\text{COO})_2$ ratios (R_c): $R_c = 0.5$ (a), 1 (b), 2 (c), 4 (d); water to ethanol ratio (R_s) = 100/100; dropping rate 3.4 ml min^{-1} ; reflux time 1 hour.

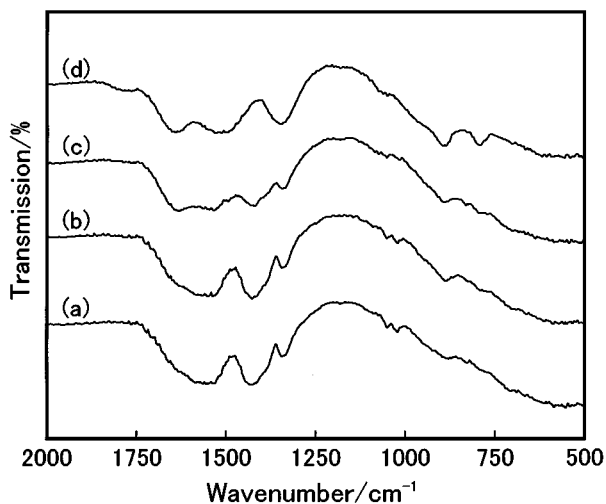


Figure 2 IR spectra for the products: $R_c = 0.5$ (a), 1 (b), 2 (c), 4 (d); $R_s = 100/100$; dropping rate 3.4 ml min^{-1} ; reflux time 1 hour.

Fig. 2 demonstrates IR spectra for the products with changing Rc. Two peaks located at 890 and 795 cm^{-1} are due to the OH bending of goethite. These two peaks were clearly observed in the top curve ($R_c = 4$), but were ambiguous in the other three curves. It is clear that goethite was precipitated for the particles prepared at $R_c = 4$. Four peaks located around 1300 to 1600 cm^{-1} were attributed to various types of acetate anions. It is well known that acetate ion adsorbs on iron oxide to form varieties of surface species such as mononuclear monodentate, mononuclear bidentate and binuclear complexes [15]. Infrared bands due to these three complexes appear at 1320 cm^{-1} , 1425 and 1520 cm^{-1} , and 1425 and 1600 cm^{-1} , respectively. Two peaks located at 1425 and 1600 cm^{-1} decreased with an increase of Rc. On the other hand, the intensity of two peaks at 1320 and 1520 cm^{-1} was not remarkably changed. Therefore binuclear complexes are easily decomposed by the attack of the OH^- ion, while acetate ligands of

mononuclear configuration strongly bind to the surface of precipitates.

The DTA-TG curve showed that acetate groups in adsorbed species calculated from the weight loss were less than 5% for the product prepared under the conditions of $R_s = 100/100$ and $R_c = 2$. The molar ratio of acetate anions to iron ($\text{CH}_3\text{COO}/\text{Fe}$) evaluated from the results of the DTA-TG curve and elemental analysis was calculated to be 0.03 for the above product, and it increased with a decrease of R_c .

In alkaline aqueous solution, ferrihydrite transforms into hematite or goethite under different conditions. Ferrihydrite is converted to hematite by the solid state reaction in which dehydration and rearrangement processes lead to the nucleation and growth of hematite involves. In contrast, goethite is generated by the dissolution of ferrihydrite. The transformation of ferrihydrite into hematite begins in denser areas of ferrihydrite aggregates because the crystal structure of hematite is very similar to that of ferrihydrite. Goethite is readily formed from ferrihydrite at pH 12–14 since ferrihydrite dissolves to form soluble monomeric species ($\text{Fe}(\text{OH})_4^-$) in alkaline media.

Acetoxy groups chemically adsorbed on the surface of precipitated particles induced ferrihydrite aggregates, indicating that the aggregates accelerated hematite formation as compared with the goethite one. Fisher *et al.* reported that hematite crystals were grown within the aggregates after hematite nuclei were generated in ferrihydrite aggregates; eventually, hematite crystallite size becomes similar to that of the initial aggregates [16]. Similar results were obtained in the present study: the crystallite size of hematite particles calculated from XRD patterns increased with increasing adsorbing ligands.

A small amount of goethite particles was formed in a water-ethanol mixture at $R_c = 4$. The dissolution rate of ferrihydrite is higher in stronger alkaline media until pH 14. Goethite is in particular formed in aqueous solution at pH 12–14 when the temperature is over 70 °C [17]. In our study, hematite was synthesized in ethanolic solutions whose pH were above 12. This result suggests that ethanol retarded goethite formation. Studies have shown that ferric ions may complex with ethanol [18]. Surface chelate such as the acetoxy group also suppresses the dissolution of ferrihydrite. In our study, goethite was formed only for the precipitate prepared at $R_c = 4$, the level of adsorbed acetate ions was less compared with other precipitates. The preparation condition at $R_c = 4$ is not suitable for preparing fine spherical hematite particles because needle-like goethite is barely converted to spherical hematite. In the solution of $R_s = 100/100$, the best ratio of NaOH against $\text{FeOH}(\text{CH}_3\text{COO})_2$ (R_c) for preparing suitable particles was 2.

3.2. Solvent effect

Fig. 3 shows XRD patterns of the products prepared at $R_c = 2$ in different media: $R_s = 0/200$ (a), 100/100 (b), and 200/0 (c). Two broad peaks located at $2\theta = 35$ and 62 degrees are similar to those of 2-line ferrihydrite in the pattern (a). In the pattern (b), broad peaks and sharp

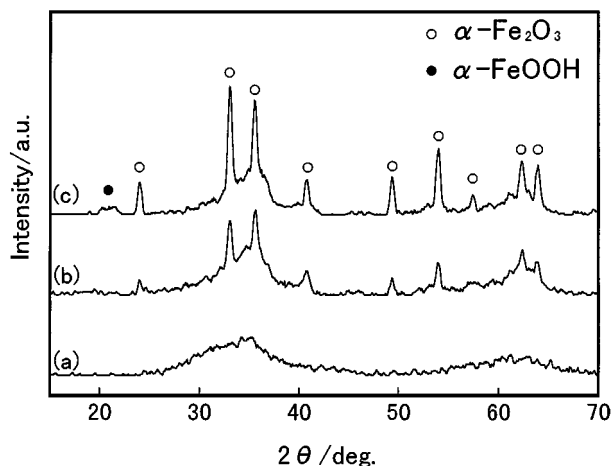


Figure 3 XRD patterns of the products prepared in different media: $R_s = 0/200$ (a), 100/100 (b), 200/0 (c); $R_c = 2$; dropping rate 3.4 ml min^{-1} ; reflux time 1 hour.

peaks are seen, which are attributed to ferrihydrite and hematite, respectively. In the pattern (c), the small peak at $2\theta = 21$ degrees, which was assigned to the main peak of goethite ($hkl = 110$), is observed together with the peaks of ferrihydrite and hematite. The hematite peaks become sharper as water content in the media is increased. Using the Scherrer equation, the calculated crystallite size of hematite from the sharp peak of 35 degree ($hkl = 104$) were 15 and 24 nm for the products prepared at $R_s = 100/100$ and 200/0, respectively.

Fig. 4 shows TEM bright-field images of the product prepared at $R_c = 2$ in different media: $R_s = 0/200$ (a); 100/100 (b); 200/0 (c). Fine particles less than 5 nm in diameter, attributed to 2-line ferrihydrite, are shown in Fig. 4a. The TEM micrograph in Fig. 4b shows spherical particles 5–10 nm in diameter. In view of the many sharp peaks in Fig. 3b, the particles are assumed to be hematite. Although the mean diameter (ca. 8 nm) of hematite particles observed in Fig. 4b is slightly smaller than that of the crystallite size (15 nm) calculated from the peak (104) in Fig. 3b, the particles are probably hematite single crystal. Three particles shown in Fig. 4c were needle-like, fine (less than 5 nm), and large spherical (20–40 nm); they were assumed to be goethite, ferrihydrite, and hematite, respectively. As shown in Fig. 3c, goethite crystals were produced under the condition at $R_s = 200/0$.

Karin reported that the transformation rate of ferrihydrite into hematite rises with reaction temperature [19]. The particle size of hematite crystallite prepared at $R_s = 200/0$ was 3–4 times larger than that at $R_s = 100/100$, since reflux temperatures of the solutions at $R_s = 200/0$ and 100/100 were 98 °C and 90 °C, respectively.

The transformation of goethite from ferrihydrite involves the dissolution of ferrihydrite in alkaline media [20]. Because surface chelate on ferrihydrite particles depresses the solubility of ferrihydrite in media, only a small amount of goethite particles was precipitated at $R_s = 0/200$; this was owing to the small amount of adsorbing acetate ions on the particles compared with other particles. Ethanol and propenol affect the rate of precipitation of goethite as well as the mechanism of

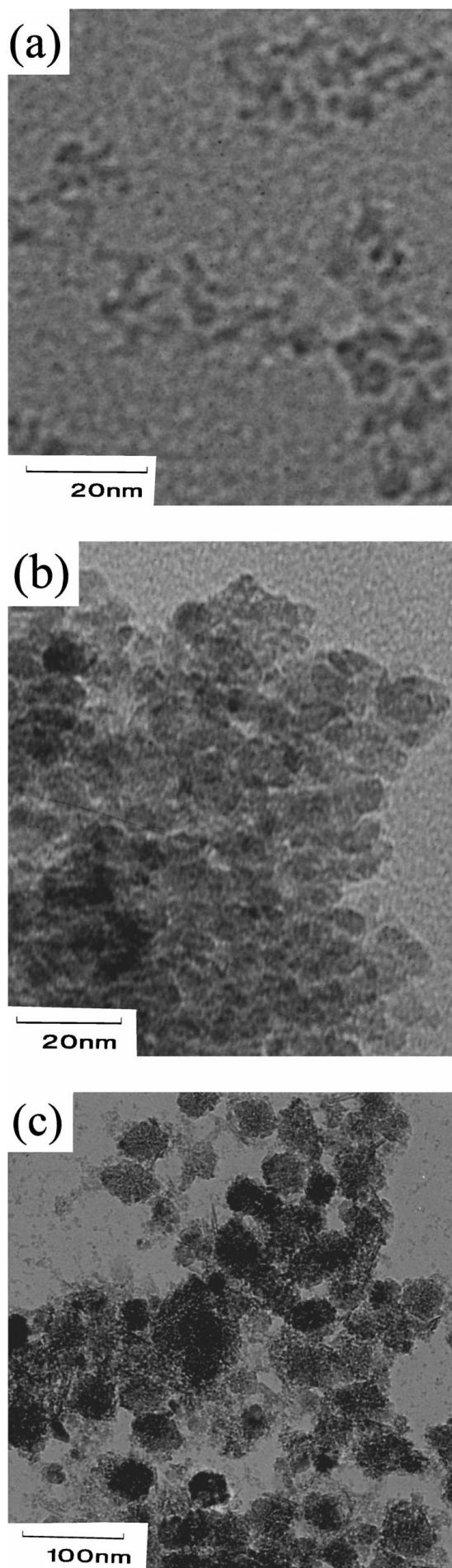


Figure 4 TEM bright-field images of the products prepared in different media: $R_s = 0/200$ (a), $100/100$ (b), $200/0$ (c); $R_c = 2$; dropping rate 3.4 ml min^{-1} ; reflux time 1 hour.

precipitation; they also influence the aging of goethite [21]. In this study, ethanol retarded the aging of goethite to hematite, and also suppressed the conversion of ferrihydrite to hematite, and also suppressed the generation of needle-like goethite particles. Furthermore, no hematite was precipitated under the preparation condition at $R_s = 200/0$ as shown in Fig. 3a. Therefore the solution at $R_s = 100/100$ prefers to prepare fine hematite particles.

3.3. Effect of dropping rate

Fig. 5 presents TEM photographs of the products prepared under the condition of $R_c = 2$ and $R_s = 100/100$ at different dropping rates for the addition of NaOH-solution: 200 ml min^{-1} (a) and 1.7 ml min^{-1} (b). Fine particles of ferrihydrite of less than 5 nm in diameter are shown in Fig. 5a. The formation of ferrihydrite nuclei involves three stages: nucleophilic attack of OH^- ions on iron (III) ions, formation of an Fe-OH bond and a dehydration-condensation reaction to form an oxo linkage (Fe-O-Fe). In our study, the addition of NaOH solution induced an instantaneous nucleophilic reaction to form Fe-OH, resulting in a good deal of ferrihydrite nuclei. Two particles, whose diameters were less than 5 nm and 30–50 nm, respectively, are seen in Fig. 5b. The former particles were assumed to ferrihydrite, and the latter hematite. Hematite particles appear much larger in Fig. 5b than in Fig. 4b. The gradual addition of NaOH solution produced a reduced amount of nuclei, and results in the growth of hematite particles. Therefore, we conclude that the dropping rate strongly affected hematite particle size.

3.4. Effect of aging time

Fig. 6 shows the XRD patterns of the products at different reflux times. Precipitates were obtained under the following conditions: $R_s = 100/100$; $R_c = 2$; dropping rate = 200 ml min^{-1} . Hematite and/or ferrihydrite were generated in the products under all conditions. Broad goethite peaks were observed in the top two patterns (24 h and 48 h). Hematite peaks became sharper as aging time increased, suggesting that hematite nanocrystallites grew gradually. After 48 hours, the crystallite size of hematite nanocrystals were several tens of nanometers of particle diameter as estimated from the hematite (104) peak. In another study, hematite crystal prepared in $4\text{M } [\text{OH}^-]$ aqueous solution at 80°C was several microns in diameter [9], approximately 100 times larger than that prepared in this experiment. Therefore, we may conclude that, in our study, adsorbing ligands such as acetate anion and ethanol strongly obstructed the transformation of ferrihydrite into hematite. The peak intensity of ferrihydrite particles decreased with continued aging, while hematite peaks became sharper. These results suggest that a large amount of ferrihydrite particles generated at an early stage did not become larger, but were converted to hematite particles. Goethite crystals gradually grew into detectable size for XRD measurement after 48 hours' aging; ferrihydrite seemed to dissolve moderately to form goethite particles under the preparation conditions: $R_s = 100/100$; $R_c = 2$.

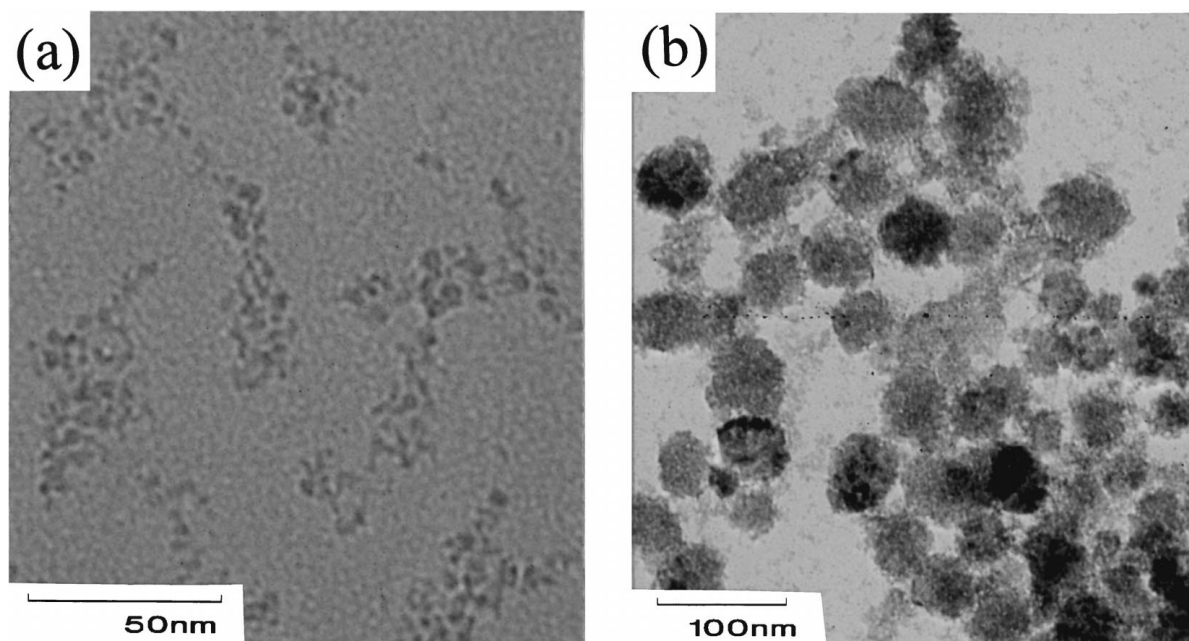


Figure 5 TEM photographs for the products prepared under the condition of $R_s = 100/100$, $R_c = 2$ and 1 hour of reflux time at different dropping rate for pouring NaOH-solution: 200 ml min^{-1} (a) and 1.67 ml min^{-1} (b).

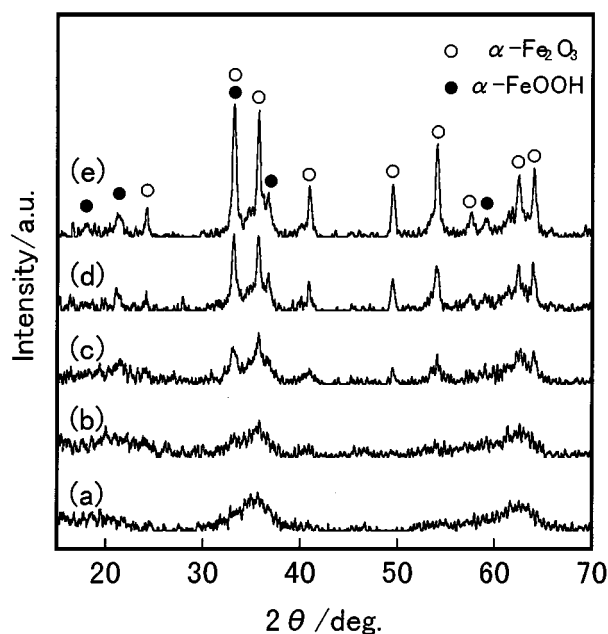


Figure 6 XRD patterns of the products prepared at $R_s = 100/100$, $R_c = 2$ and 3.4 ml min^{-1} of dropping rate for different reflux times: 1 h (a); 4 h (b); 12 h (c); 24 h (d); 48 h (e).

Fig. 7 shows change in specific surface area of as-prepared particles against reflux time. Specific surface area steeply decreased as aging time increased. The large specific surface area of the particles aged for 1, 2, and 4 hours was caused mainly by fine ferrihydrite particles. Thus the reduction of the surface area indicates the transformation of ferrihydrite into hematite during reflux. The crystallite size calculated from specific surface area of the particles aged for 24 hours was several nanometers, which was nearly ten times smaller than that calculated from the Sherrer equation using the hematite (104) peak. The main reason for this is probably the existence of fine ferrihydrite particles, although

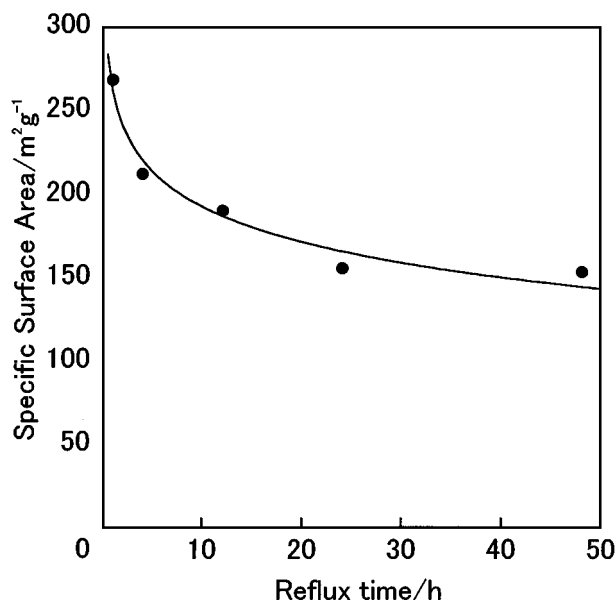


Figure 7 Change in specific surface area of the particles against reflux time.

the broad peaks attributed to ferrihydrite are diminished in Fig. 6d.

3.5. Heat treatment

A reddish-brown powder was obtained after as-prepared particles were heated under an air stream to eliminate organic residue. Fig. 8a shows a TEM micrograph of the particles, which were prepared in the following conditions: $R_s = 100/100$; $R_c = 2$; dropping time 3.4 ml min^{-1} , heated at 400°C for 2 hours. Heated particles appeared to be spherical and monomodal (ca. 20 nm in diameter), and were assumed to be hematite by their XRD pattern. No ferrihydrite existed in the heated particles because fine particles (less than 5 nm) were not observed in the micrograph. There was

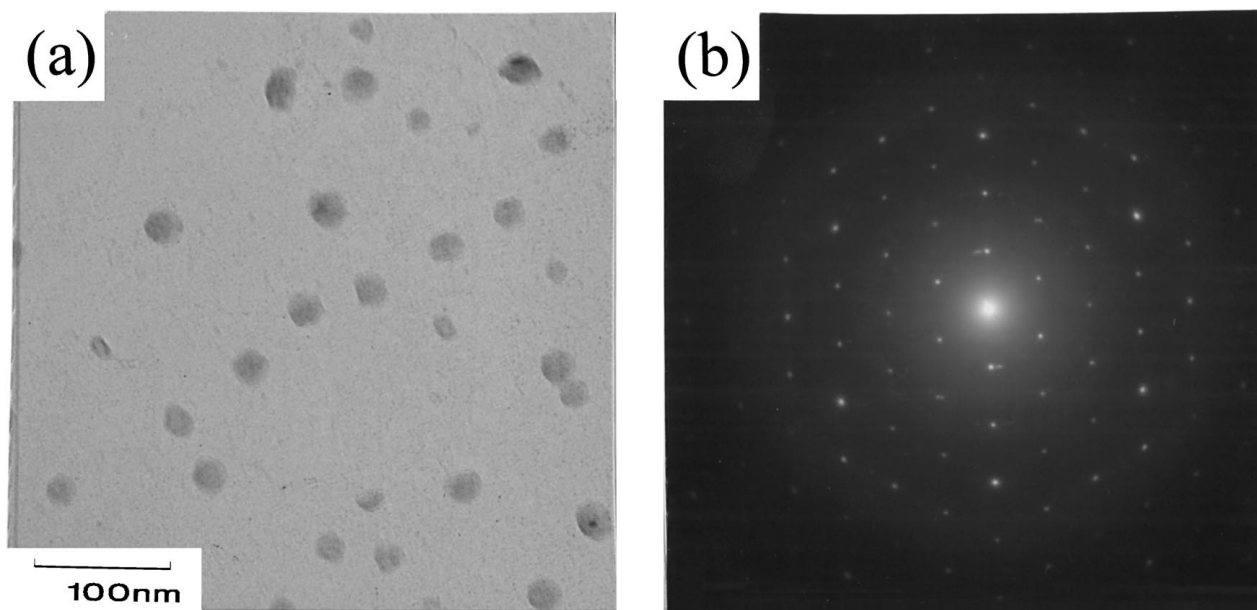


Figure 8 TEM micrograph of the particles heated at 400 °C for 2 hours (a) and selected electron diffraction pattern for a predetermined particle (b).

also no peak due to ferrihydrite for the XRD pattern of heated particles. The particle size was comparable to that calculated from the hematite (104) peak. Specific surface area of the particles was $118 \text{ m}^2 \text{ g}^{-1}$. Aggregated hematite particles of as-prepared precipitates were released during heating because the remaining organics on the surface of as-prepared particles were combusted. Fine ferrihydrite particles were adsorbed on hematite particles to form larger spherical hematite particles. The selected electron diffraction pattern for a predetermined particle was shown in Fig. 8b. This diffraction pattern indicates that the particle was monocrystalline and the surface of the particle, to which the electron beam was incident, was the (001) plane of hexagonal structure.

Figure 9 shows the histogram of size distribution for the heated particles. The average particle size

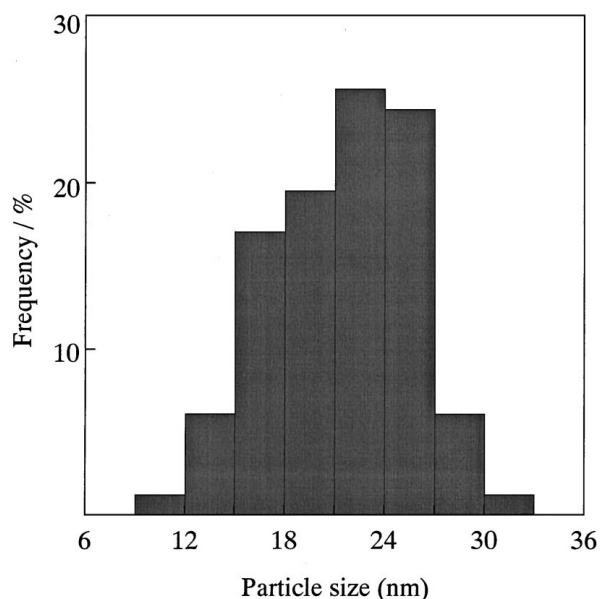


Figure 9 Histogram of size distribution for the heated particles at 400 °C for 2 hours.

was 22 nm in diameter with a narrow size distribution ($\delta = 4.2 \text{ nm}$); no irregular grown particle existed. Carlson reported that the DTA curve of ferrihydrite has a sharp exothermic peak around 300 °C which is due to the transformation of highly disordered hematite into ordered hematite [22]. Towe found that 6-line ferrihydrite was completely converted to hematite after heat treatment at 400 °C for 1 hour [23]. Structural rearrangement of ferrihydrite adsorbed on nanometer-sized hematite particles was initiated during heating at 400 °C for 2 hours, leading to nano-sized hematite single crystals. Furthermore high surface area of the as-prepared particles ($285 \text{ m}^2 \text{ g}^{-1}$) is a possible cause of further ordering [24].

After the heat treatment of ferrihydrite particles prepared at $R_s = 0/200$, the particles were converted to hematite polycrystalline with broad size distribution. Since there was no hematite nanocrystallite to serve as nuclei, single hematite crystals were not formed. Agglomeration of ferrihydrite particles with each other during heating presumably induced broad size distribution. For the particles prepared at $R_s = 200/0$, needle particles remained after heating.

4. Conclusion

We have demonstrated that nanometer-sized spherical hematite single crystals (mean particle size: 22 nm) were synthesized by heat treatment of the precipitates at 400 °C for 2 hours: the precipitates were prepared in an ethanol-water solution without deliberate addition of surfactants and or absorbing ligands.

Ferrihydrite and hematite were precipitated in alkaline ethanol-water mixture ($R_s = 100/100$), while ferrihydrite was produced in ethanol under all of the same conditions except the media. Needle-like goethite particles as well as hematite and ferrihydrite were precipitated at $R_s = 200/0$. Ethanol obscured the transformation of ferrihydrite into hematite. Alkaline media accelerated the formation of goethite particles even in

ethanolic solution. Fine ferrihydrite particles were prepared in ethanol-water mixture by immediate addition of NaOH solution. Spherical hematite single crystals were produced by heat treatment at 400 °C from the particles precipitated in the ethanol-water mixture, but only ferrihydrite particles were converted to hematite polycrystalline with broad size distribution during heating.

Acknowledgement

This work was supported in part by the Collaborative Research Project of the Materials and Structures Laboratory, Tokyo Institute of Technology.

References

1. S. CHATTERJEE, S. SARKAR and N. BHATTACHARYYA, *J. Photochem. Photobiol. A: Chem.* **72** (1993) 183.
2. C. PULGARIN and J. KIWI, *Langmuir* **11** (1995) 519.
3. E. MATIJEVIC and P. SCHEINER, *J. Colloid Interface Sci.* **63** (1978) 509.
4. S. HAMADA and E. MATIJEVIC, *J. Chem. Soc. Faraday Trans.* **78** (1982) 2147.
5. E. MATIJEVIC and S. CIMAS, *Colloid & Polymer Sci.* **265** (1987) 155.
6. K. KANDORI, A. YASUKAWA and T. ISHIKAWA, *J. Colloid Interface Sci.* **180** (1996) 446.
7. T. SUGIMOTO and A. MURAMATSU, *ibid.* **184** (1996) 626.
8. N. J. REEVES and S. MANN, *J. Chem. Soc. Faraday Trans. I* **87** (1991) 3875.
9. R. M. CORNELL and R. GIOVANOLI, *Clays Clay Min.* **35** (1987) 11.
10. R. S. SAPIEZKO and E. MATIJEVIC, *J. Colloid Interface Sci.* **74** (1980) 405.
11. S. KAN, S. YU, X. OENG, X. ZHANG, D. LI, L. XIANG, G. ZOU and T. LI, *ibid.* **178** (1996) 673.
12. U. SCHWERTMANN and R. M. CORNELL, "Iron Oxides in the Laboratory" (VCH, Weinheim, 1991) p. 137.
13. D. BRANDL, CH. SHOPPMANN, CH. TOMASCHKO, J. MARKL and H. VOIT, *Thin Solid Films* **249** (1994) 113.
14. M. GAO, X. PENG and J. SHEN, *ibid.* **248** (1994) 106.
15. A. D. BUCKLAND, C. H. ROCHESTER and S. A. TOPHAM, *J. Chem. Soc. Faraday Trans. I* **76** (1980) 302.
16. W. R. FISHER and U. SCHWERTMANN, *Clays Clay Min.* **23** (1975) 33.
17. R. M. CORNELL and R. GIOVANOLI, *ibid.* **33** (1985) 219.
18. S. HAMADA and E. MATIJEVIC, *J. Colloid Interface Sci.* **84** (1981) 274.
19. Z. KARIN, *Clays Clay Min.* **32** (1984) 181.
20. U. SCHWERTMANN and E. MURAD, *ibid.* **31** (1983) 277.
21. J. TORRENT and U. SCHWERTMANN, *J. Sediment. Petrology* **57** (1987) 682.
22. L. CARLSON and U. SCHWERTMANN, *Geochim. Cosmochim. Acta* **45** (1980) 421.
23. K. M. TOWE, "Origin, Evolution, and Modern Aspects of Biomineralization in Plants and Animals" (Plenum Press, New York, 1990) p. 265.
24. F. WATARI, P. DELAVIGNETTE, V. J. LAMDUYT and S. AMELINCKZ, *J. Solid State Chem.* **48** (1983) 49.
25. M. IWASAKI, Y. INUBUSHI and S. ITO, *J. Mater. Sci. Lett.* **16** (1997) 1503.
26. Y. INUBUSHI, R. TAKAMI, M. IWASAKI, H. TADA and S. ITO, *J. Colloid Interface Sci.* **200** (1998) 220.
27. M. IWASAKI, M. HARA and S. ITO, *J. Mater. Sci. Lett.* **17** (1998) 1769.

Received 13 January
and accepted 22 July 1999